NANO LETTERS
2005
Vol. 5, No. 5
981−984

Size-dependent Photoconductivity in MBE-Grown GaN–Nanowires

Raffaella Calarco,* Michel Marso, Thomas Richter, Ali I. Aykanat, Ralph Meijers, André v.d. Hart, Toma Stoica, and Hans LUth

Institute of Thin Films and Interfaces (ISG1) and cni - Center of Nanoelectronic Systems for Information Technology, Research Centre Jülich, 52425 Jülich, Germany

Received January 6, 2005; Revised Manuscript Received March 15, 2005

ABSTRACT

We report on electrical transport in the dark and under ultraviolet (UV) illumination through GaN nanowhiskers grown by molecular beam epitaxy (MBE), which is sensitively dependent on the column diameter. This new effect is quantitatively described by a size dependent surface recombination mechanism. The essential ingredient for the interpretation of this effect is a diameter dependent recombination barrier, which arises from the interplay between column diameter and space charge layer extension at the column surface.

The bottom-up approach to growing nanowires (whiskers) in several semiconductor material systems (Si,[1] III−V,[2−6] III-nitride[7−9]) with the aim of quantum electronic, optoelectronic, and sensor applications has attracted considerable interest worldwide. Even though sophisticated device structures such as RTDs, SETs, field effect transistors, biosensors, and even logic gates could already be realized by these self-organized nanowires,[10−15] many fundamental questions about the internal electronic structure, the effect of the large surface in comparison to its bulk, and size dependent transport phenomena remain unanswered up to now.

In this context our investigation of MBE-grown GaN nanowires demonstrates, for the first time to our knowledge, the effect of surface Fermi-level pinning[16] and its interplay with the nanowire dimensions on the recombination behavior of electron−hole pairs in photoconductivity through these wires.

Due to surface Fermi-level pinning within the forbidden band, GaN wires, as do most other semiconductor wires, exhibit a depletion space charge layer with an extension of the order of the wire diameter. Depending on wire thickness and doping, completely depleted wires or wires with thin conducting channels exist. Depending on the applied voltage, charge limited currents, characteristic for insulators, or ohmic behavior is observed. These effects are explicitly obvious under light-induced carrier excitation. In corresponding photoconductivity experiments, therefore, photoexcited electrons and holes are more or less spatially separated from each other depending on the extension of the surface space charge layer in comparison with the wire diameter. When surface recombination of nonequilibrium electron−hole pairs through surface traps is the prevailing mechanism, then the recombination rate and therefore also the absolute amount of the photocurrent density should depend very sensitively on the wire diameter. This is indeed found in the present investigations.

The GaN nanowires are grown by radio frequency plasma-assisted MBE on Si(111) substrates. The whisker density and diameter, 20−500 nm, are controlled by means of the III/V ratio. Below stoichiometry (defined as the III/V ratio at which the growth rate saturates) the epitaxial growth proceeds nominally under N-rich conditions, which leads to the desired columnar morphologies. The growth conditions are described elsewhere.[17] For a detailed experimental description of the growth mechanisms see the extensive work of Calleja et al.[8]

After epitaxial growth, the nanowires are released from the native Si(111) substrate by exposure to an ultrasonic bath and deposited on a Si(100) host substrate covered with an insulation layer of 300 nm SiO_2. Ti(10 nm)/Au(100 nm) contacts patterned by electron beam lithography allow the electrical and optoelectrical characterization of the nanowires (Figure 1). To check for possible surface effects on the transport measurements due to atmosphere, the first investigations were performed under a vacuum of 10^{-5} mbar, but no difference to measurements in atmosphere were found.

Figure 2 shows the results of photoconductivity measurements for nanowires with three different thicknesses d: 500 nm, 190 nm, and 70 nm. Their behavior concerning photocurrent decay after UV illumination is completely different. For relatively thick wires (d > 200 nm) in the dark, currents between 10^{-6} A and 10^{-5} A are measured in both voltage polarities. After illumination with UV light by a mercury−xenon lamp via a quartz fiber (approximately 15 W/cm^2), a photocurrent higher by slightly an order of magnitude is observed. After switching off the light the photocurrent

* Corresponding author. E-mail: r.calarco@fz-juelich.de.

10.1021/nl0500306 CCC: $30.25
Published on Web 03/22/2005

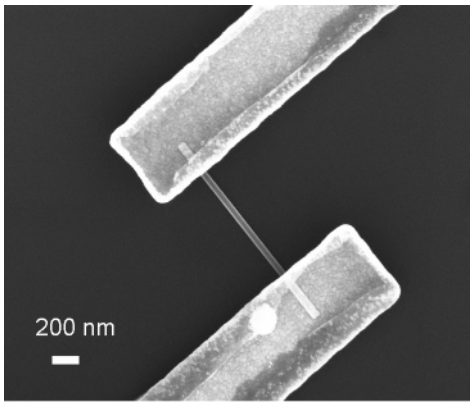

Figure 1. SEM picture of a nanowire on Si host substrate, with Ti/Au contact electrodes. Nanowire diameter: 70 nm.

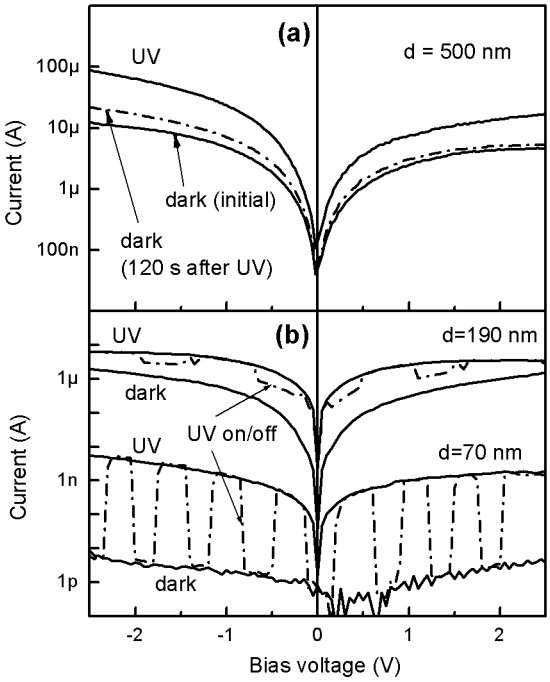

Figure 2. Current−voltage characteristics of GaN nanowires with different diameters with and without UV illumination. (a) 500 nm sample, dark and under steady-state UV illumination. (b) 190 nm and 70 nm samples, dark and under steady-state UV illumination, as well as under periodic UV illumination (dash−dotted). The behavior of the current after switching off the light (persistent photoconductivity) depends on the diameter.

decays fast, but not to the dark current value; it rather stays as a persistent photocurrent (in the dark), even 120 s after the end of the illumination at approximately double the dark current value (Figure 2a). This effect of a persistent photocurrent is observed for wires with diameters down to about 100 nm. For the example in Figure 2b with $d = 190$ nm the photocurrent upon UV illumination decreases each time when the light is switched off for some short period $\Delta t = 1-2$ s, but does not reach the dark current value. A considerable current persists in the dark periods. The effect is also clearly seen from the time transient of the photocurrent in the 500 nm sample (Figure 3), where even after 5 min the current exceeds the initial dark value by about 3×10^{-6}A.

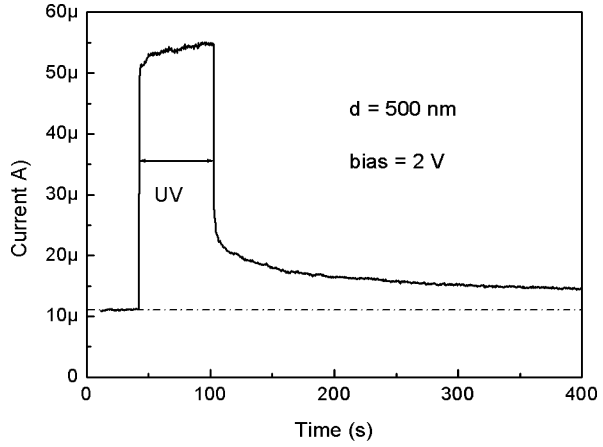

Figure 3. Current transient after 1 min of UV illumination (15 W/cm^2) of the 500 nm sample.

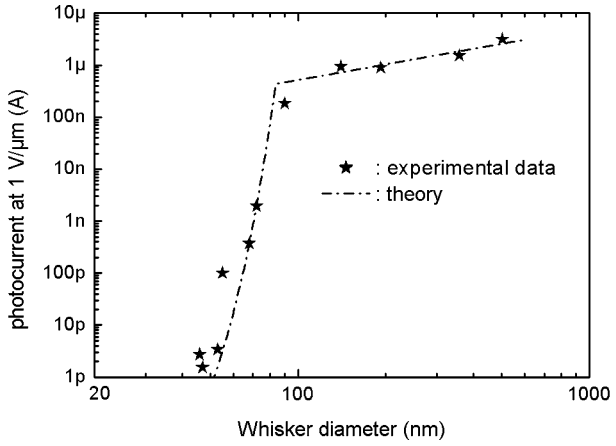

Figure 4. Photocurrent with UV illumination of approximately 15 W/cm^2 versus whisker diameter. The kink in the fitting curve at 85 nm indicates the critical diameter d_{crit}, where the surface depletion layer just completely depletes the nanowire. For smaller diameters the photocurrent shows an exponential decrease, for larger diameters the photocurrent is proportional to the wire diameter.

Thinner wires with diameters below about 100 nm (see example in Figure 2b with $d = 70$ nm), in contrast, exhibit a fast photoresponse. For the 70 nm sample the maximum observed photocurrents reach values at around 10^{-8} A. Control experiments have shown that the measured dark current of this sample is a parasitic background current not related to transport through the GaN column. Photocurrents in these thin GaN columns decay rapidly in the dark, which demonstrates that there is no persistent photocurrent anymore. Such a fast photoresponse was also observed by Han et al.[18] on 15 nm thin GaN nanowires, but without an interpretation of the effect.

This general pattern of size dependent photocurrents is also clearly seen when one plots the measured photocurrent (as additive to dark current or parasitic background), at a bias voltage of about 1 V; more precisely, an electric field of 1 V/μm, to account for different electrode spacings, versus GaN nanowire diameter (Figure 4). While for wire diameters above 100 nm the photocurrent changes only slightly with diameter, below approximately 80 nm a sharp drop to immeasurable values is observed.

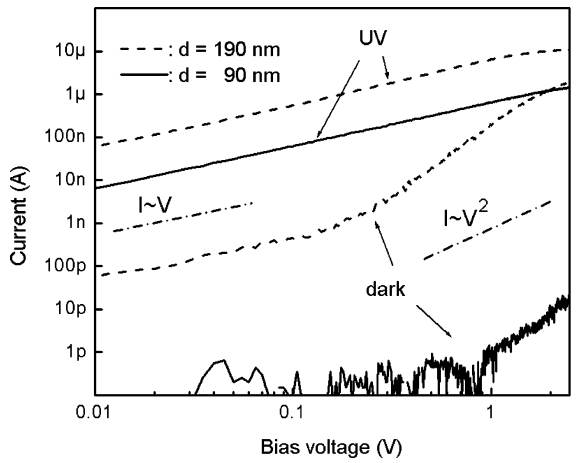

Figure 5. Double logarithmic plot of the current−voltage characteristic for samples with different diameters. For comparison $I \propto V$ and $I \propto V^2$ dependences are given in dash−dotted line. The photocurrent (UV) shows ohmic behavior, while the dark current turns into a V^2 to V^3 voltage dependence at bias voltages above 0.1 V. This behavior is characteristic for space charge limited currents in insulators. (The dark current of the thin nanowire is below the measurement limit for voltages below 1 V).

A double logarithmic plot of the current−voltage characteristics (Figure 5) is helpful for a better understanding of the phenomena. For the 190 nm sample, the photocurrent under stationary illumination follows essentially a linear dependence on bias voltage, as is expected for ohmic behavior of a conducting channel in the whisker. Furthermore, this ohmic behavior, which is also found for the 500 nm thick sample in Figure 2a, both in the dark and with UV illumination (at least up to 0.4 V), clearly demonstrates that the contacts are largely ohmic and that effects due to Schottky barriers at the contacts can be neglected. This is expected from literature data for Ti/Au contacts.[19] However, the dark current, 3 orders of magnitude below the photocurrent at bias voltages between 0.01 and 0.1 V, turns into a V^2 to V^3 voltage dependence at bias voltages above 0.1 V. This behavior is characteristic for space charge limited currents in insulators.[20] A similar effect is also observed for the 90 nm column. The photocurrent is essentially linear (ohmic) in voltage, while the dark current is below the measurement limit for voltages below 1 V and then shows a space charge limited current behavior.

From the observation of space charge limited currents we conclude that dark and photocurrents in these GaN columns are governed by depletion space charge layers, which are due to Fermi-level pinning at the surface of the nanocolumns. From previous photoemission spectroscopy studies on GaN surfaces, Fermi-level pinning is expected at about 0.5−0.6 eV below the conduction band edge.[21] Assuming an n-type background doping in the 10^{17}cm^{-3} range, the depletion space charge layers should have extensions of 50 to 100 nm into the bulk. Depending on the column diameter the whiskers, therefore, are completely depleted at small diameters (<80 nm) or have a tight open conducting channel at diameters above 100 nm. But even under those conditions the columns are essentially insulators in the dark due to their depletion space charge layers. Dark currents, at least for diameters

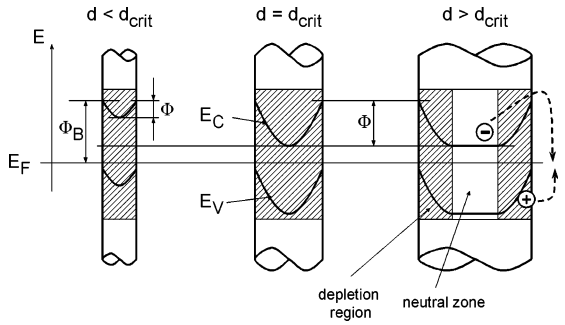

Figure 6. Dependence of depletion region (shaded), shape of conduction (E_C) and valence band edges (E_V), and recombination barrier Φ on the nanowire diameter d. The relative energetic locations of E_C, E_V, and E_F are not on scale. The detail on the right shows the surface recombination mechanism of the photoexcited carriers.

below 200 nm, are space charge limited, as is characteristic for insulators. Only the higher carrier densities under UV light illumination allow ohmic behavior for diameters above 100 nm.

The existence of depletion space charge layers at the column surface also explains the size dependent photocurrent behavior (Figs. 2, 4) quantitatively.

Because of Fermi-level pinning at the surface, the electronic bands, conduction (E_C) and valence (E_V), are bent upward at the surface of the n-doped column as shown schematically in Figure 6. Electrons prefer the inner part of the column, whereas holes tend to move to the surface. Due to their spatial separation, recombination of nonequilibrium carriers is thus reduced or is maybe even impossible if recombination via surface traps in the forbidden band is the prevailing recombination mechanism. Electrons would have to surpass the conduction band barrier at the surface for surface recombination. This model of hindered surface recombination due to the presence of depletion space charge layers explains the persistent photocurrent for columns with diameters above 100 nm (Figures 2 and 3). As is seen qualitatively from Figure 6, a decrease of the column diameter leads to complete depletion (detail in the middle) at a critical diameter d_{crit} with unchanged surface barrier height Φ for electrons in the conduction band. Down to this critical diameter, the recombination rate, i.e., also the photocurrent, does not change significantly. Further shrinking of the dimensions, however, causes less band curvature and therefore a reduction of the barrier for surface electron−hole pair recombination (Figure 6, detail on the left). With decreasing thickness now the recombination process is strongly enhanced and the photocurrent decays strongly with decreasing barrier height, i.e., with decreasing column thickness.

This model thus explains that the photocurrent remains on a relatively high level as long as the column diameters exceed the critical value around 80 to 100 nm, where the column is completely depleted. Below this critical diameter surface barriers are diminished and the photocurrent drops steadily due to enhanced surface recombination (Figure 6).

The following assumptions allow a quantitative model description for the observed size dependent photoconductiv-

ity. (i) The nanocolumns behave like a photoconductor without Schottky-contacts at the metallization. (ii) The optical absorption length for photons is much larger than the column diameter, such that photoexcitation is homogeneous all over the sample. (iii) Photogenerated carriers do not significantly affect the potential, i.e., the band structure within the column. (iv) The time decay of the persistent photocurrent is essentially due to surface recombination, where holes are pushed to the surface due to the surface band bending and electrons have to overcome the corresponding surface barrier (Figure 6) in order to recombine. Under these conditions we calculate the stationary photocurrent from the balance between generation rate (proportional to absorption constant, column volume, and irradiated light intensity) and surface recombination rate (proportional to column surface and recombination rate). The recombination rate is essentially given by an exponential term $\exp(-\phi/kT)$, where the barrier for electrons to recombine with holes amounts to

$$\phi = eN_D d^2/16\epsilon\epsilon_0 \text{ for } d < d_{crit} \quad (1a)$$

$$\phi = eN_D d^2_{crit}/16\epsilon\epsilon_0 \text{ for } d > d_{crit} \quad (1b)$$

For $d > d_{crit}$ (minimum diameter for a fully depleted column) a constant barrier height (eq 1b) with N_D as donor concentration and $\epsilon\epsilon_0$ as dielectric constant of GaN causes a nearly constant (slightly varying) photocurrent (proportional to column diameter), as is observed in the experiment (Figure 4). For column diameters $d < d_{crit}$, the recombination barrier ϕ depends quadratically on the column diameter d (eq 1a) and gives rise to a sharp exponential drop of the photocurrent.

The described theoretical model yields a nearly perfect fit to the measured data (Figure 4). Three fitting parameters are obtained numerically. One parameter, essentially the proportionality factor between the photocurrent and the exponential decay term, contains details about the electron−hole pair generation mechanism, which are not well-known so far. The second fitting parameter, the donor concentration N_D, is obtained as $N_D = 6.25 \times 10^{17}\text{cm}^{-3}$. This N_D value corresponds well with doping levels obtained under standard MBE conditions for GaN layers. It is worth emphasizing that the unintentional doping in nanocolumns is obviously not different from that during layer growth. Because of different growth conditions for columns (N-rich) and layers (Ga-rich), one would expect different dopant incorporation. The third fitting parameter, the barrier height ϕ_B at diameters above d_{crit} (eq 1b), follows as 0.55 eV. This barrier value corresponds very well to the surface potential ($E_C - E_F$) (see Figure 6), which has been determined to be between 0.5 and 0.6 eV [21] from photoemission spectroscopy (XPS) on clean GaN layers. More details about the experiments and the theoretical analysis will be given in a subsequent, more extended paper.

In conclusion, our model of surface electron−hole pair recombination excellently describes the unusual behavior of size dependent persistent photocurrents in GaN nanocolumns. The physical bases of the effect are size dependent recombination barriers within the whiskers, which are due to the interplay between column diameter and space charge extension.

The described effects are of general importance for all kinds of semiconductor nanowires, electronic transport through these structures, and in particular applications of nanowires in optoelectronics and sensor technology.

References

(1) Lauhon, L.; Gudiksen, M.; Wang, D.; Lieber, C. *Nature* **2002**, *420*, 57.
(2) Gudiksen, M.; Lauhon, L.; Wang, J.; Smith, D.; Lieber, C. *Nature* **2002**, *415*, 617.
(3) Wang, J.; Gudiksen, M.; Duan, X.; Cui, Y.; Lieber, C. *Science* **2001**, *293*, 1455.
(4) Hiruma, K.; Yazawa, M.; Haraguchi, K.; Ogawa, K.; Katsuyama, T.; Koguchi, M.; Kakibayashi, H. *J. Appl. Phys.* **1993**, *74*, 3162.
(5) Ohlsson, B.; Björk, M.; Magnusson, M.; Deppert, K.; Samuelson, L.; Wallenberg, L. *Appl. Phys. Lett.* **2001**, *79*, 3335.
(6) Ohlsson, B.; Björk, M.; Persson, A.; Thelander, C.; Wallenberg, L.; Magnusson, M.; Deppert, K.; Samuelson, L. *Physica E* **2002**, *13*, 1126.
(7) Sánchez-Páramo, J.; Calleja, J.; Sánchez-Garcia, M.; Calleja, E.; Jahn, U. *Physica E* **2002**, *13*, 1070.
(8) Calleja, E.; Sánchez-Garcia, M.; Sánchez, F.; Calle, F.; Naranjo, F.; Muñoz, E.; Jahn, U.; Ploog, K. *Phys. Rev. B* **2000**, *62*, 16826.
(9) Ristic, J.; Calleja, E.; Sánchez-Garcia, M.; Ulloa, J.; Sánchez-Páramo, J.; Calleja, J.; Jahn, U.; Trampert, A.; Ploog, K. *Phys. Rev. B* **2003**, *68*, 125305.
(10) Thelander, C.; Mårtensson, T.; Björk, M.; Ohlsson, B.; Larsson, M.; Wallenberg, L.; Samuelson, L. *Appl. Phys. Lett.* **2003**, *83*, 2052.
(11) Greytak, A.; Lauhon, L.; Gudiksen, M.; Lieber, C. *Appl. Phys. Lett.* **2004**, *84*, 4176.
(12) Duan, X.; Huang, Y.; Agarwal, R.; Lieber, C. *Nature* **2003**, *421*, 241.
(13) Zhong, Z.; Wang, D.; Cui, Y.; Bockrath, M.; Lieber, C. *Science* **2003**, *302*, 1377.
(14) Björk, M.; Ohlsson, B.; Thelander, C.; Persson, A.; Deppert, K.; Wallenberg, L.; Samuelson, L. *Appl. Phys. Lett.* **2002**, *81*, 4458.
(15) Björk, M.; Ohlsson, B.; Sass, T.; Persson, A.; Thelander, C.; Magnusson, M.; Deppert, K.; Wallenberg, L.; Samuelson, L. *Appl. Phys. Lett.* **2002**, *80*, 1058.
(16) Lüth, H. *Solid Surfaces, Interfaces and Thin Films*, 4th ed.; Springer: Berlin, Heidelberg, 2001; Chapter 7.
(17) Calarco, R.; Marso, M.; Meijers, R.; Richter, T.; Aykanat, A. I.; Stoica, T.; Lüth, H. *Proceedings of the ASDAM '04 Conference*, Smolenice, Slovakia, **2004**, 9.
(18) Han, S.; Jin, W.; Zhang, D.; Tang, T.; Li, C.; Liu, X.; Liu, Z.; Lei, B.; Zhou, C. *Chem. Phys. Lett.* **2004**, *389*, 176.
(19) Schmitz, A. C.; Ping, A. T.; Khan, M. A.; Chen, Q.; Yang, J. W.; Adesida, I. *Semicond. Sci. Technol.* **1996**, *11*, 1464.
(20) Rose, A. *Phys. Rev.* **1955**, *97*, 1538.
(21) Kočan, M.; Rizzi, A.; Lüth, H.; Keller, S.; Mishra, U. K. *Phys. Status Solidi B* **2002**, *234*, 773.

NL0500306